

Reliability analysis of load-sharing systems with memory

Dewei Wang¹  · Chendi Jiang¹ ·
Chanseok Park²

Received: 1 January 2017 / Accepted: 15 February 2018
© Springer Science+Business Media, LLC, part of Springer Nature 2018

Abstract The load-sharing model has been studied since the early 1940s to account for the stochastic dependence of components in a parallel system. It assumes that, as components fail one by one, the total workload applied to the system is shared by the remaining components and thus affects their performance. Such dependent systems have been studied in many engineering applications which include but are not limited to fiber composites, manufacturing, power plants, workload analysis of computing, software and hardware reliability, etc. Many statistical models have been proposed to analyze the impact of each redistribution of the workload; i.e., the changes on the hazard rate of each remaining component. However, they do not consider how long a surviving component has worked for prior to the redistribution. We name such load-sharing models as *memoryless*. To remedy this potential limitation, we propose a general framework for load-sharing models that account for the work history. Through simulation studies, we show that an inappropriate use of the memoryless assumption could lead to inaccurate inference on the impact of redistribution. Further, a real-data example of plasma display devices is analyzed to illustrate our methods.

Keywords Load-share parameters · Maximum likelihood estimator · Parallel system · lifetime prediction · System dependence

Electronic supplementary material The online version of this article (<https://doi.org/10.1007/s10985-018-9425-8>) contains supplementary material, which is available to authorized users.

✉ Dewei Wang
deweiwang@stat.sc.edu

¹ Department of Statistics, University of South Carolina, Columbia, SC 29208, USA

² Department of Industrial Engineering, Pusan National University, Busan, Korea

1 Introduction

The load-sharing model is commonly used to analyze the reliability of a parallel system which consists of multiple identical components. In this system, all the components are connected parallel to share the total workload. Such reliability systems are widely applied in real applications. For example, electric generators are organized in parallel in a power plant to share the electrical load; cables are connected in parallel to undertake the stress of a suspension bridge. In these systems, components eventually fail one by one. As a failure occurs, the load taken by the failed component will be redistributed to the remaining components and hence affects their lifetime distribution.

To account for the load-share process, various load-sharing rules have been proposed. Daniels (1945) described how the break-up of an individual fiber could increase the strain on others within a bundle. Because the threads of fibers are of equal length and clamped at each end, it is natural to assume that all the threads have the same load-extension till the occurrence of a breakpoint. The assumption of equal load-extension has been adopted again in Coleman (1957a, b), Rosen (1964). This common assumption, that all the functional components are sharing the same amount of load, is referred to as *the equal load-sharing rule*. Other load-sharing rules have also been studied in the literature. We refer readers to Birnbaum and Saunders (1958), Harlow and Phoenix (1978), Phoenix (1978), Phoenix and Tierney (1983), Lee et al. (1995), Harlow (1997), Durham et al. (1997). In this article, we proceed under the equal load-sharing rule. Extending the method to other load-sharing rules is not difficult.

Under the equal load-sharing rule, Kim and Kvam (2004) provided a pioneering work to make the parametric inference of the reliability of the system. The lifetime of individual components is assumed to be exponentially distributed; i.e., the individual hazard rate is constant. Singh et al. (2008) relaxed the assumption of constant rate and considered that after a certain number of component failures, the hazard rates increase linearly in time. Park (2010) considered a more general load-sharing model which contains the models of Kim and Kvam (2004), Singh et al. (2008) as special cases. The maximum likelihood estimators are studied under both exponential and Weibull distributions. Further, Park (2013) developed an expectation-maximization algorithm that can handle a larger class of distributions in a computationally efficient fashion. Besides parametric methods, nonparametric reliability analysis has also been studied; see, e.g., Kvam and Peña (2005).

All the aforementioned works assume that, after each component failure, the lifetime of surviving components follow a new distribution regardless of how long they have already worked for. We characterize load-sharing models under this assumption as *memoryless*. However, this memoryless assumption may not be reasonable in practice. For example, let us consider two identical and independent load-sharing systems. Suppose the first failure in the first system occurs much later than the one in the second system. Memoryless load-sharing models suggest that the remaining components in both systems have the same lifetime distribution, even the remaining components in the first system have worked for a longer time; i.e., accumulated more hazard or suffered from more stress. By doing so, the ignored hazard or stress are then forced to be taken into account by parameters that are used to model the impact of the workload redistribution. Consequently, it would overestimate those parameters. In this article,

our goal is to make the first attempt to help practitioners obtain correct inference on the reliability by tracking the hazard accumulated on surviving components prior to each failure.

Towards this end, we start with a general framework in Sect. 2. This framework is built by characterizing the lifetime distribution of functioning components between each two consecutive failures. We focus on two perspectives: the potential impact of a workload redistribution and the hazard accumulated till the redistribution. Various models, such as the Hawkes process (Hawkes 1971) or the Cox proportional hazard model (Cox 1972), could be used as special cases under our general framework. In order to analytically track the cumulated hazard, Sect. 3 focuses on two approaches. The first one measures hazard using the total time that components have worked for. After a failure occurred, as long as the surviving components have worked for the same amount of time, the distributions of their remaining lifetime are identical. We name models of this type by *load-sharing models with recent memory*. The second one uses cumulative hazard functions (CDF) to sequentially track the full work history of each component. We name models of the second type by *load-sharing models with full memory*. In Sect. 4, a general likelihood function is provided for defining the maximum likelihood estimator (MLE). The likelihood could be applied to any parametric hazard rate functions. The estimator enjoys asymptotic normality as expected. We further illustrate the generality by considering Weibull, gamma, log-normal, and Gompertz distributions in Sect. 5. Detailed algorithms for data generation, a method for finding initial values to compute, and a final search for the MLE are included in the web-based supplementary materials. Numerical results reveal the consequence of ignoring cumulated hazard prior to each component failure. A real data set is analyzed to reveal the advances of our approaches in Sect. 6. Sect. 7 concludes the article with a discussion. R codes are available in the web-based supplementary materials.

2 The general model

Consider a parallel system of size J , where the size is defined to be the number of components in the system. We assume that the system works under a constant load and the equal load-sharing rule applies throughout. That is, at any time, the entire load is distributed equally to the functioning components. As time goes by, components eventually fail one by one. We do not consider replacing or repairing failed components. However, designing an effective maintenance plan could be an interesting future topic (see Sect. 7). Let S_j be the time when the j th failure occurs, where $j = 1, \dots, J$. We assume that the J failures occur at distinctive moments and the whole system stops after all the J components fail. In other words, we can observe all the S_j 's and $0 = S_0 < S_1 < S_2 < \dots < S_J < \infty$. We say that the system is at the j th stage when it is between S_{j-1} and S_j , for $j = 1, \dots, J$.

In the first stage, all components are functioning. Denote the lifetime of each component by U_{1k} , $k = 1, \dots, J$. Since the J components are working in parallel to share the same amount of load, we assume that U_{11}, \dots, U_{1J} are independent and identically distributed (iid) random variables with a hazard rate function $\lambda_1(u)$ for $u \in (0, \infty)$. We call $\lambda_1(\cdot)$ the initial hazard rate of a load-sharing system of size J . Of course, the

first failure occurs at time $S_1 = T_1 = \min\{U_{11}, \dots, U_{1J}\}$. It is worthwhile to point out that the purpose of this section is to generally describe our model of load-sharing systems. The notation we used in this section are kept as general as possible. For example, the initial hazard rate $\lambda_1(\cdot)$ may involve some unknown parameters, say θ ; i.e., more accurately, $\lambda_1(\cdot)$ should be written as $\lambda_1(\cdot|\theta)$. Such notation will be discussed in Sect. 4.

Once S_1 occurs, the second stage begins. The entire workload is immediately redistributed to the remaining $J - 1$ components. This redistribution might affect the lifetime distribution of each surviving component. Denote $\{U_{2k}, k = 1, \dots, J - 1\}$ to be the *remaining* lifetime of the $J - 1$ components. Under the equal load-sharing rule, we do not use the subscript k to label each component. In other words, our notation does not force the first failed component to be the J th one. We assume that, given T_1 , $\{U_{21}, \dots, U_{2,J-1}\}$ are iid with the hazard rate being $\lambda_2(u | T_1)$ for $u \in (0, \infty)$. The length of the second stage of the system is then $T_2 = \min\{U_{21}, \dots, U_{2,J-1}\}$ and $S_2 = S_1 + T_2$.

When the j th stage starts; i.e., after the $(j - 1)$ th component failure at S_{j-1} , we denote the remaining lifetime of the $J - j + 1$ functioning components by $\{U_{jk}, k = 1, \dots, J - j + 1\}$. Similarly, we assume that, given (T_1, \dots, T_{j-1}) , $\{U_{j1}, \dots, U_{j,J-j+1}\}$ are iid random variables with the hazard rate function being $\lambda_j(u | T_1, \dots, T_{j-1})$ for $u \in (0, \infty)$. Then the length of the j th stage of the system is $T_j = \min\{U_{j1}, \dots, U_{j,J-j+1}\}$ and $S_j = S_{j-1} + T_j = \sum_{l=1}^j T_l$. We name the vector $(T_1, \dots, T_{j-1})^\top$ as the work history of the $J - j + 1$ components. The reliability of the system entirely depends on the J hazard rate functions; i.e.,

$$\begin{aligned}
 &\text{Stage 1 : } T_1 = \min\{U_{11}, \dots, U_{1J}\}, \text{ where } U_{11}, \dots, U_{1J} \stackrel{iid}{\sim} \lambda_1(u), u > 0; \\
 &\quad \vdots \\
 &\text{Stage } j : T_j = \min\{U_{j1}, \dots, U_{j,J-j+1}\}, \tag{1} \\
 &\quad \text{where } U_{j1}, \dots, U_{j,J-j+1} | (T_1, \dots, T_{j-1}) \stackrel{iid}{\sim} \lambda_j(u | T_1, \dots, T_{j-1}), u > 0; \\
 &\quad \vdots \\
 &\text{Stage } J : T_J = U_{J1}, \text{ where } U_{J1} | T_1, \dots, T_{J-1} \stackrel{iid}{\sim} \lambda_J(u | T_1, \dots, T_{J-1}), u > 0,
 \end{aligned}$$

where $U_1, \dots, U_k \stackrel{iid}{\sim} \lambda(\cdot)$ means U_1, \dots, U_k are iid random variables with the hazard rate function λ . The notation $\lambda_j(\cdot | T_1, \dots, T_{j-1})$ involves two levels of meaning. First, we let $\lambda_j(\cdot)$ change with j to account for the impact from the redistribution of workload. Second, the term (T_1, \dots, T_{j-1}) allows us to incorporate the work history of the remaining components.

This general framework in (1) includes many meaningful models as special cases. For example, one could view each redistribution of workload as an arrival of event that would affect the rate of the rest reloading. This is similar to the “self-exciting” feature of the seminal Hawkes process proposed by Hawkes (1971). This process has been used for modeling the arrivals of earthquakes (Hawkes and Adamopoulos

1973; Ogata 1998), gang violence (Mohler et al. 2011), trade orders (Fonseca and Zaatour 2014), or bank defaults (Aït-Sahalia et al. 2015). The term “self-exciting” means that each arrival in the process would increase the rate of future arrivals for a certain amount of time. Learning from this idea, one could set $\lambda_j(u \mid T_1, \dots, T_{j-1}) = \lambda_1(u + S_{j-1}) + \sum_{l=1}^{j-1} v^*(u + S_{j-1} - S_l)$, for $u > 0$ and $j \geq 2$, where $v^*(\cdot)$ plays the same role as the “self-exciting” function in Hawkes processes and $u + S_{j-1} - S_l$ accounts for the impact of the l th arrival (redistribution) to the current status. Another interesting design of λ_j ’s is to apply the popular Cox proportional hazard model (Cox 1972); i.e., $\lambda_j(u \mid T_1, \dots, T_{j-1}) = \lambda_1(u) \exp(v_{j0} + v_{j1}T_1 + \dots + v_{j,j-1}T_{j-1})$ for $u > 0$ and $j \geq 2$, where v_{jk} ’s are some unknown constants that could be sequentially estimated. These examples could yield fruitful research surrounding parallel systems. In the next section, we focus a new design of λ_j ’s due to its great ability in tracking the hazard accumulated in each stage.

3 A specific design

Denote $r_j(u)$ to be the initial hazard rate of a load-sharing system of size $J - j + 1$ for $j = 1, \dots, J$. Our new design consists of the following hazard rate functions. For $u > 0$, we let

$$\lambda_1(u) = r_1(u) \text{ and } \lambda_j(u \mid T_1, \dots, T_{j-1}) = r_j(u + \kappa_j(T_1, \dots, T_{j-1})), \quad (2)$$

where $j = 2, \dots, J$, and κ_j is a j -dimensional non-negative function. The term κ_j ’s accounts for the work history that could impact the individual hazard rate after the $(j - 1)$ th failure.

Obviously, the simplest configuration of κ_j ’s would be

$$\kappa_j(T_1, \dots, T_{j-1}) = 0, \text{ for } j = 2, \dots, J; \quad (3)$$

i.e., the work history does not affect the lifetime distribution of remaining components at all. This new model includes existing models as special cases as aforementioned in Sect. 1. For example, Kim and Kvam (2004) set $\lambda_1(\cdot) = \theta$ and $\lambda_j(\cdot \mid T_1, \dots, T_{j-1}) = \gamma_j\theta$ for $j = 2, \dots, J$; Kvam and Peña (2005) set $\lambda_j(u \mid T_1, \dots, T_{j-1}) = \gamma_j\lambda_1(u)$ for $j = 2, \dots, J$ where $\lambda_1(u)$ is a smooth unknown function. Singh et al. (2008) considered the same setting as in Kim and Kvam (2004) but $\lambda_j(u \mid T_1, \dots, T_{j-1}) = \gamma_j\theta u$ when j gets larger than a certain number s . More generally, Park (2010, 2013) considered and $\lambda_j(u \mid T_1, \dots, T_{j-1}) = \lambda_j(u)$ for $j > 1$, where $\lambda_j(u)$ are unknown up to several parameters. In all these studies, the work history affects nothing to the hazard rate of the next stage. We name such models with (3) as *memoryless load-sharing models* (MLSM). Using the term “memoryless” does not force all the individual lifetime U_{jk} ’s to be exponentially distributed. It only means that κ_j ’s are zero.

The first row of Fig. 1 plots an example to illustrate the hazard rates of a MLSM. In this example, the load-sharing system consists of three components. The three component failures occurred at time S_1, S_2 , and S_3 . The length of the first, second,

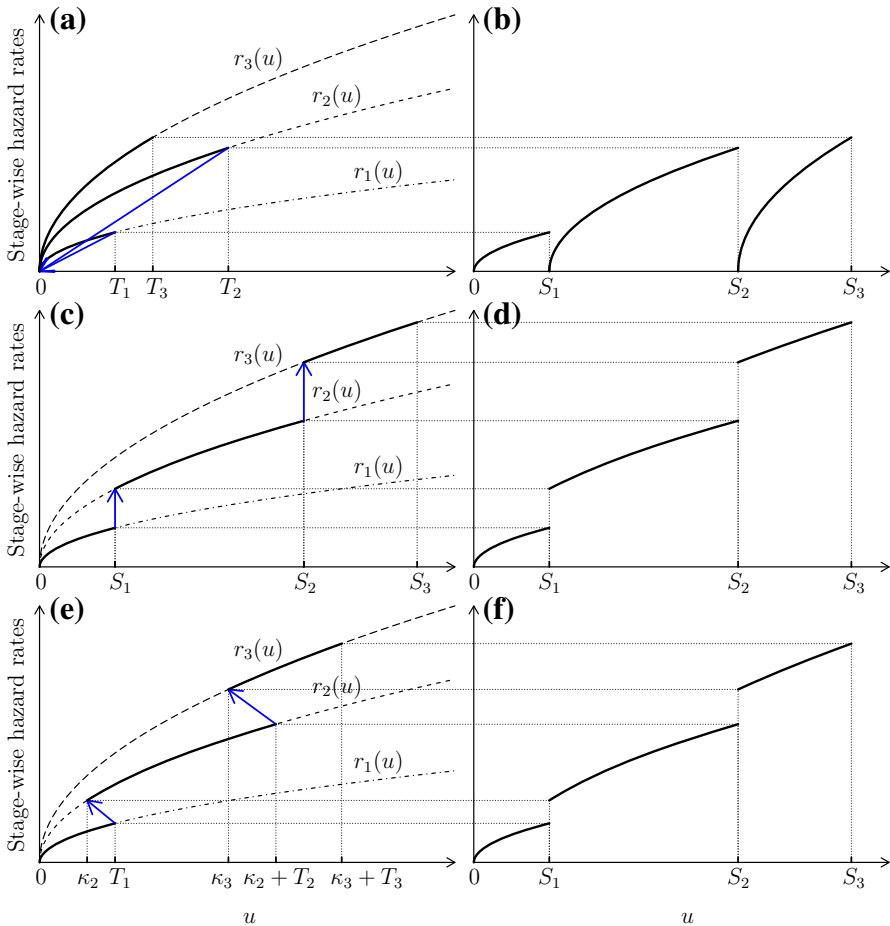


Fig. 1 An illustration of the construction of the hazard rate for each stage under the MLSM (the first row), the LSMRM (the second row), and the LSMFM (the last row) for a load-sharing system of size 3. The three component failure times are $S_1 = T_1$, $S_2 = S_1 + T_2$, and $S_3 = S_2 + T_3$. Arrows are used to show how each model considers the work history. Part (a) describes how the MLSM ignores the work history and the resulting observed hazard rates are plotted in part (b). Part (c) describes how the LSMRM considers the work history and part (d) summarizes the resulting hazard rates. Part (e) describes how the LSMFM tracks the work history, in which we write $\kappa_2 = \kappa_2(T_1)$ and $\kappa_3 = \kappa_3(T_1, T_2)$ for notational simplicity, and part (f) displays the resulting hazard rates

and last stage are $T_1 = S_1$, $T_2 = S_2 - S_1$, and $T_3 = S_3 - S_2$, respectively. In the first stage. All three components worked under the hazard rate $r_1(u)$ from the starting time $u = 0$ to T_1 . At T_1 , the workload was reloaded to two components. With two components undertaking all, the individual hazard rate was boosted from $r_1(\cdot)$ to $r_2(\cdot)$. However, regardless of the fact that the two components have already worked for time T_1 , the MLSM assumes that the second stage should be counted from 0 to T_2 under the curve $r_2(\cdot)$. Similarly, for the last stage, the MLSM assumes that the hazard rate corresponding to the remaining lifetime of the last component should be counted from 0 to T_3 under $r_3(\cdot)$, no matter how large S_2 is. The arrows in Fig. 1a highlight how the

work history is ignored, and Fig. 1b summarizes the observed hazard rates concluded by the MLSM.

In order to incorporate the work history, we propose two approaches. The first one sets

$$\kappa_j(T_1, \dots, T_{j-1}) = \sum_{l=1}^{j-1} T_l; \tag{4}$$

i.e., $\lambda_j(u \mid T_1, \dots, T_{j-1}) = r_j(u + \sum_{l=1}^{j-1} T_l)$ for $j = 2, \dots, J$. It is because that, after the $(j - 1)$ th failure, all the surviving components have already worked for time $\sum_{l=1}^{j-1} T_l$. We name the model in (4) as *load-sharing models with recent memory* (LSMRM). The word “recent” means that the function κ_j is related only with the work history $(T_1, \dots, T_{j-1})^\top$ by the summation $\sum_{l=1}^{j-1} T_l$ regardless of how much hazards were accumulated in each stage.

The second row of Fig. 1 illustrates how hazard rates are constructed in a LSMRM. When the first component failure happened at time $S_1 = T_1$, the individual hazard rate was increased from $r_1(\cdot)$ to $r_2(\cdot)$. Because the remaining components have already worked for time S_1 , their hazard rates in Stage 2 are counted from S_1 to S_2 under curve $r_2(\cdot)$, rather than from 0 to T_2 in the MLSM. Similarly, the hazard rate of the functioning component in Stage 3 started from $r_3(S_2)$ and ended at $r_3(S_3)$. The arrows in Fig. 1c indicate that how the previous work times are considered in the LSMRM, and Fig. 1d plots the corresponding observed hazard rates.

Now a natural question arises. Suppose we have two identical and independent load-sharing systems A and B , both of which are of size three. We denote the lengths of the first and second stages of system A to be T_{A1} and T_{A2} , respectively, and denote those of system B to be T_{B1} and T_{B2} , respectively. Consider the case that T_{A1} is much larger than T_{B1} but $T_{A1} + T_{A2}$ and $T_{B1} + T_{B2}$ are equal (or very close). Under the LSMRM assumption, the last component in both systems should have the same hazard rate function. However, prior to the second failure, a large proportion of time of the last component in A was spent when the load was shared by three components, while in B was spent with only two components. Thus, the hazard rate of the last component in A should be less than the one in B . Such difference cannot be reflected by the LSMRM.

Our second choice of κ_j 's is designed to track the cumulated hazard sequentially. The last row of Fig. 1 explains the essential idea. The initial stage remains the same; i.e., every component worked from 0 to the first component failure time T_1 under hazard rate $r_1(\cdot)$. The differences appear at the beginning of Stage 2. Let $R_j(t) = \int_0^t r_j(u)du, t > 0$; i.e., the cumulative hazard function corresponding to the hazard rate $r_j(\cdot)$. Rather than counting from 0 to T_2 in the MLSM, or from S_1 to S_2 in the LSMRM, we count from $\kappa_2(T_1)$ to $\kappa_2(T_1) + T_2$, where $\kappa_2(T_1)$ satisfies $R_2(\kappa_2(T_1)) = R_1(T_1)$; i.e., the area under $r_1(u)$ from 0 to T_1 is the same as the area under $r_2(\cdot)$ from 0 to $\kappa_2(T_1)$, or equivalently,

$$\kappa_2(T_1) = R_2^{-1}(R_1(T_1)).$$

In other words, working from 0 to T_1 under $r_1(\cdot)$ is the same as working from 0 to $\kappa_2(T_1)$ under $r_2(\cdot)$. At the moment S_2 , the cumulated hazard of the only surviving component is then $R_1(T_1) + R_2(\kappa_2(T_1) + T_2) - R_2(\kappa_2(T_1)) = R_2(\kappa_2(T_1) + T_2)$.

Consequently, one could think that the last component has worked from time 0 to time $\kappa_3(T_1, T_2)$ under $r_3(\cdot)$, where

$$\kappa_3(T_1, T_2) = R_3^{-1}(R_2(\kappa_2(T_1) + T_2)).$$

Thus, the observed length of Stage 3 should be counted starting from $\kappa_3(T_1, T_2)$ and ending at $\kappa_3(T_1, T_2) + T_3$. The arrows in Fig. 1e illustrates how to track the cumulated hazard step by step, and Fig. 1f plots the hazard rates based on the observed values of S_1 , S_2 , and S_3 .

In general, one could sequentially construct our final choice of κ_j 's with

$$\kappa_j(T_1, \dots, T_{j-1}) = R_j^{-1}(R_{j-1}(\kappa_{j-1}(T_1, \dots, T_{j-2}) + T_{j-1})). \quad (5)$$

To ensure the existence of the inverse of R_j , we assume that $r_j(\cdot)$'s are positive differentiable functions, which is a mild assumption in reliability analysis. For load-sharing models characterized by (5), we name them by *load-sharing models with full memory* (LSMFM).

We recognize that the construction of (5) shares a similar spirit with the cumulative exposure model proposed by Nelson (1980) for the step-stress accelerated life testing. We refer readers to Zhao and Elsayed (2005) and references therein for more detailed discussion. Herein, we would like to point out that the time to change the stress in the step-stress model is fixed by designers before the experiment, while in our scenario, the redistribution of the workload occurs randomly in terms of which working component is and when it fails; i.e., S_1, \dots, S_J are random. Such randomness further increases the difficulty for estimation.

4 Estimation

In order to keep the maximum flexibility of our approach, we assume that each individual hazard rate function $r_j(\cdot)$ involves unknown parameters. Collect all unknown parameters into a vector β and denote the length of β by p . For notational convenience, we rewrite $r_j(\cdot) = r_j(\cdot | \beta)$ for $j = 1, \dots, J$, and the true memory configuration $\kappa_j(T_1, \dots, T_{j-1}) = \kappa_j(T_1, \dots, T_{j-1} | \beta)$ for $j = 2, \dots, J$. For example, models in Kim and Kvam (2004) and Singh et al. (2008) can be summarized by

$$r_1(\cdot) = r_1(\cdot | \theta), \text{ and } r_j(\cdot) = \gamma_j r_1(\cdot | \theta), \text{ for } j = 2, \dots, J, \quad (6)$$

where parameter θ defines the initial individual hazard rate $r_1(\cdot)$ and $\gamma = (\gamma_2, \dots, \gamma_J)^\top$ is a vector of the the load-share parameters that characterizes the impact of each redistribution of workload. In this case, we have $\beta = (\theta^\top, \gamma^\top)^\top$.

To estimate β , we first derive the joint probability density function of (T_1, \dots, T_J) using hazard rates introduced in (2). It is easy to see that

$$\text{pr}_\beta(T_1 > t) = \prod_{k=1}^J \text{pr}_\beta(U_{1k} > t) = \exp \left\{ -J \int_0^t r_1(u | \beta) du \right\},$$

which yields the marginal probability density function of T_1 being

$$f_{T_1}(t | \beta) = Jr_1(t | \beta) \exp \left\{ -J \int_0^t r_1(u | \beta) du \right\}.$$

For $j \geq 2$, we have

$$\begin{aligned} & \text{pr}_\beta(T_j > t | T_1 = t_1, \dots, T_{j-1} = t_{j-1}) \\ &= \prod_{k=1}^{J-j+1} \text{pr}_\beta(U_{jk} > t | T_{i1} = t_1, \dots, T_{i,j-1} = t_{j-1}) \\ &= \exp \left[-(J - j + 1) \int_0^t r_j(u + \kappa_j(t_1, \dots, t_{j-1} | \beta) | \beta) du \right]. \end{aligned}$$

Then, the conditional probability density function of T_j given $(T_1 = t_1, \dots, T_{j-1} = t_{j-1})$ is

$$\begin{aligned} & f_{T_j|T_1=t_1, \dots, T_{j-1}=t_{j-1}}(t | \beta) = (J - j + 1)r_j(t + \kappa_j(t_1, \dots, t_{j-1} | \beta) | \beta) \\ & \times \exp \left[-(J - j + 1) \int_0^t r_j(u + \kappa_j(t_1, \dots, t_{j-1} | \beta) | \beta) du \right]. \end{aligned}$$

for $j = 2, \dots, J$. Finally, the joint probability density function of (T_1, \dots, T_J) is

$$\begin{aligned} f(t_1, \dots, t_J | \beta) &= J! \prod_{j=1}^J \left(r_j(t_j + \kappa_j(t_1, \dots, t_{j-1} | \beta) | \beta) \right. \\ & \left. \times \exp \left[-(J - j + 1) \int_0^{t_j} r_j(u + \kappa_j(t_1, \dots, t_{j-1} | \beta) | \beta) du \right] \right) \quad (7) \end{aligned}$$

where $t_j > 0$ for $j = 1, \dots, J$ and $\kappa_1 = 0$.

Suppose that we observe n independent and identically-distributed load-sharing systems of size J until all systems fail. We record all the component failures of each system by $\{0 = S_{i0} < S_{i1} < S_{i2} < \dots < S_{iJ} < \infty, i = 1, \dots, n\}$, where S_{ij} is the j th component failure time of the i th system. Denote $T_{ij} = S_{ij} - S_{i,j-1}$ for $j = 1, \dots, J$. Then using (7), we can write the log-likelihood function by

$$\begin{aligned} \ell_n(\beta) &= n \log(J!) + \sum_{i=1}^n \sum_{j=1}^J \log r_j(T_{ij} + \kappa_j(T_{i1}, \dots, T_{i,j-1} | \beta) | \beta) \\ & - \sum_{i=1}^n \sum_{j=1}^J (J - j + 1) \int_0^{T_{ij}} r_j(u + \kappa_j(T_{i1}, \dots, T_{i,j-1} | \beta) | \beta) du. \quad (8) \end{aligned}$$

Consequently, we define our estimator $\widehat{\beta}_n$ to be the maximizer of $\ell_n(\beta)$ with respect to β . The following theorem discusses the asymptotic normality of $\widehat{\beta}_n$.

Theorem 1 Denote the true value of β by β_0 . Under regularity conditions (A1)–(A3) in the Appendix, we have

$$\sqrt{n}(\widehat{\beta}_n - \beta_0) \xrightarrow{d} N(\mathbf{0}, \mathcal{I}(\beta_0)^{-1}), \text{ as } n \rightarrow \infty,$$

where \xrightarrow{d} means convergence in distribution, $\mathbf{0}$ is a vector of zeros, and $\mathcal{I}(\beta)$ is the Fisher information matrix defined in the regularity condition (A2).

The proof of Theorem 1 follows standard arguments for the asymptotic properties of maximum likelihood estimators (Lehmann 1983). For the purpose of making statistical inference, such as computing confidence intervals. It is important to obtain an estimator of the asymptotic covariance matrix. This could be done using the inverse of the Hessian matrix of the log-likelihood function; i.e.,

$$\widehat{\mathcal{I}}(\widehat{\beta}_n) = -\frac{1}{n} \frac{\partial^2 \ell_n(\beta)}{\partial \beta \partial \beta^\top} \Big|_{\beta = \widehat{\beta}_n}.$$

Based on the consistency of $\widehat{\beta}_n$, we have $\widehat{\mathcal{I}}(\widehat{\beta}_n)$ converge in probability to $\mathcal{I}(\beta_0)$ as n goes to infinity. Further, for any real-valued matrix D with rank $\tau > 0$ and number of columns being p , an asymptotic $100(1 - \alpha)\%$ confidence region of $D^\top \beta$ could be

$$\{D^\top \beta : n(\widehat{\beta}_n - \beta)^\top D \{D^\top \widehat{\mathcal{I}}(\widehat{\beta}_n)^{-1} D\}^{-1} D^\top (\widehat{\beta}_n - \beta) \leq \chi_\tau^2(\alpha)\} \quad (9)$$

where $\chi_\tau^2(\alpha)$ is the upper α th quantile of a chi-square distribution with degrees of freedom τ . Especially, an asymptotic $100(1 - \alpha)\%$ confidence region for the k th component of β could be obtained by setting D being a binary vector whose k th element is one and others are zero.

5 Numerical studies

In this section, we conduct a simulation study to explore the finite sample performance of the proposed methods. We focus on the model setting in the form of (6); i.e., the initial individual hazard rate $r_1(\cdot) = r_1(\cdot | \theta)$ and $r_j(\cdot) = \gamma_j r_1(\cdot | \theta)$ for $j > 1$. The parameters in the vector $\beta = (\theta^\top, \gamma^\top)^\top$, where $\gamma = (\gamma_2, \dots, \gamma_J)^\top$ are called the load-share parameters. We consider the following choices for the initial hazard rate $r_1(\cdot | \theta)$, where $\theta = (\theta_1, \theta_2)^\top$:

- $r_1(\cdot)$ is the hazard rate of a Weibull distribution with shape $\theta_1 = 1.5$ and scale $\theta_2 = 0.3$;
- $r_1(\cdot)$ is the hazard rate of a gamma distribution with shape $\theta_1 = 2$ and rate $\theta_2 = 10$;
- $r_1(\cdot)$ is the hazard rate of a log-normal with the log mean $\theta_1 = -1.8$ and the log standard deviation $\theta_2 = 0.5$;
- $r_1(\cdot)$ is the hazard rate of a Gompertz distribution with shape $\theta_1 = 3$ and rate $\theta_2 = 1$.

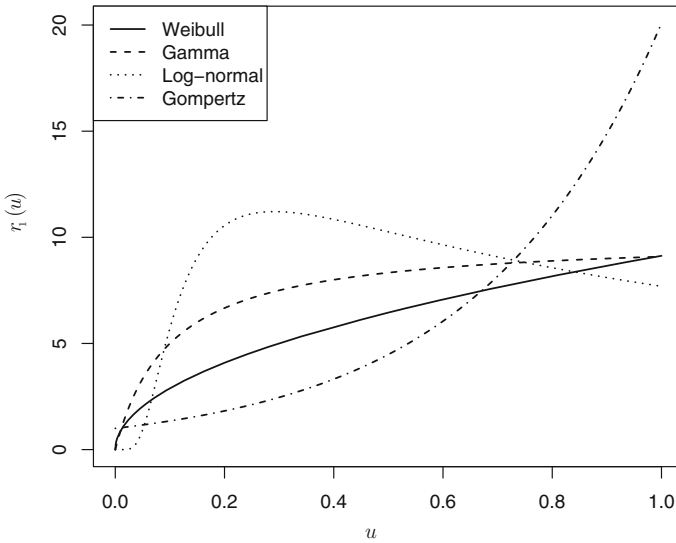


Fig. 2 The four choices of $r_1(\cdot)$ considered in Sect. 5

The shape of these choices are plotted in Fig. 2. For the load-share parameters in $\boldsymbol{\gamma}$, we consider:

- $\gamma_j = 1$ for $j = 2, \dots, J$;
- $\gamma_j = J/(J - j + 1)$ for $j = 2, \dots, J$.

The first choice of $\boldsymbol{\gamma}$ emulates the scenario in which the redistribution of workload to fewer components does not increase the hazard rate. In addition, when all γ_j 's are all one, the LSMRM and LSMFM are equivalent; i.e., (4) and (5) are the same. For the second setting for $\boldsymbol{\gamma}$, we consider the case where the monotone load-sharing rule applies; i.e., $1 \leq \gamma_2 \leq \dots \leq \gamma_J$. From each combination of $r_1(\cdot)$ and $\boldsymbol{\gamma}$, we consider $J = 3$ and generate a random sample $\{(T_{i1}, \dots, T_{i3}) : i = 1, \dots, n\}$ from the LSMFM. This allows us to investigate the consequence of an inappropriate use of the memoryless assumption. Further, when all γ_j 's are one, the LSMFM reduces to the LSMRM. We can further see the performance of the LSMRM.

We consider various sample sizes; i.e., $n \in \{50, 100, 200\}$. The data generation mechanism is included in Web Appendix A. Using each generated sample, we estimate $\boldsymbol{\beta}$ under the three model assumptions; i.e., the MLSM, the LSMRM, and the LSMFM, where estimates are obtained by maximizing (8) with κ_j 's in (3), (4), and (5), respectively. The numerical search for $\hat{\boldsymbol{\beta}}$ could be problematic if the initial values of $\boldsymbol{\beta}$ were wrongly specified. We have provided a sequential method for obtaining good initial values along with a completed set of R codes in Web Appendix B.

We repeat the process of generating samples and estimating $\boldsymbol{\beta}$ for 5000 times. Tables 1, 2, 3 and 4 provide summary statistics of the 5000 estimates of $\boldsymbol{\beta}$ obtained under each of the three models across all considered sample sizes for the Weibull and gamma distributions, respectively. Results for the log-normal and Gompertz distributions are of a similar pattern and thus included in Web Appendix C.

Recall that when $\gamma_j = 1$, for $j = 2, \dots, J$, the LSMRM and LSMFM are equivalent. From Tables 1 and 3, we see that as n increases, both methods exhibit a sharp decreasing trend in bias and MSE. The empirical coverage probabilities for 95% confidence intervals, constructed using (9), are a little off when n is small but increase to their nominal level quickly when n gets larger. Moreover, we can see the average lengths of 95% confidence intervals from the LSMRM are smaller than the ones from the LSMFM. This is reasonable since the log-likelihood function under the LSMRM is of a much simpler format; i.e., it does not have to calculate the inverse of a cumulative hazard function as in (5). The estimates under the MLSM behave poorly. For example, the empirical coverage probabilities decrease to 0 quickly as n increases. More importantly, because the MLSM does not account for the work history, it leads to large estimates of $\boldsymbol{\gamma}$ which falsely suggest a monotone load-sharing rule holds. In other words, the MLSM has to use large estimates of γ_j 's to account for the accumulated hazard prior to each component failure.

When $\gamma_j = J/(J - j + 1)$, for $j = 2, \dots, J$, a monotone load-sharing rule holds and the LSMRM and LSMFM become different. Since samples are generated from the LSMFM, the LSMFM estimators perform well as expected (see Tables 2 and 4). The LSMRM model produces nominal coverage probabilities for $\boldsymbol{\theta}$, but low ones for $\boldsymbol{\gamma}$. This pattern suggests that the LSMRM is able to well estimate the initial hazard rate $r_1(\cdot)$. However, due to its wrong specification of the work history, the LSMRM cannot correctly estimate the load-share parameter γ_j 's. The MLSM again behaves poorly for estimating $\boldsymbol{\beta}$ in every aspect. Similar patterns can be found for the log-normal and the Gompertz distributions as provided in Web Appendix C. We have also considered the cases where $J > 3$. Results are very similar so we omitted them for brevity.

6 Real data analysis

In manufacturing, electronic displays such as plasma display devices (PDPs) can be viewed as an example of load-sharing systems. Pixels are connected together to produce luminosity and PDP failure occurs when the luminosity decreases below a certain threshold. The stress changes triggered by the degradation of one area of the PDP surface can certainly affect the luminosity of other areas. Kvam and Peña (2005) provided a study where twenty PDPs were tested for luminosity degradation. On each PDP, there are three luminosity sensors spaced evenly across the device to monitor 3 different areas of the surface. The moment of each occurrence of degradation of luminosity was recorded. These failure moments can be modeled using load-sharing models. In this section, we model the data using (6). We consider $r_1(\cdot | \boldsymbol{\theta})$ to be the hazard rate function of a Weibull distribution with shape parameter θ_1 and scale parameter θ_2 . Let $\boldsymbol{\theta} = (\theta_1, \theta_2)^\top$, and $r_j(\cdot) = \gamma_j r_1(\cdot)$ for $j = 2, 3$ where $\boldsymbol{\gamma} = (\gamma_2, \gamma_3)^\top$. Our goal is to estimate $\boldsymbol{\beta} = (\boldsymbol{\theta}^\top, \boldsymbol{\gamma}^\top)^\top$.

Three models, the MLSM, LSMRM and LSMFM, are used to estimate $\boldsymbol{\beta}$. A summary of the estimates is presented in Table 5. One can see that the estimates obtained via the LSMRM and LSMFM methods are very close. The reason might be that the estimates of γ_2 and γ_3 are close to 1 and thus (4) and (5) are nearly the same. One

Table 1 Simulation results for Weibull (shape = θ_1 , scale = θ_2) and $\gamma_2 = \gamma_3 = 1$

n	Method	Measure	$\theta_1 = 1.5$	$\theta_2 = 0.3$	$\gamma_2 = 1$	$\gamma_3 = 1$
50	MLSM	Mean(MSE)	1.253(0.068)	0.331(0.002)	1.634(0.522)	1.991(1.151)
		SE(LCI)	0.081(0.318)	0.040(0.157)	0.328(1.284)	0.405(1.588)
		95% Cov	0.171	0.963	0.558	0.231
	LSMRM	Mean(MSE)	1.539(0.020)	0.297(0.001)	0.998(0.054)	0.984(0.072)
		SE(LCI)	0.131(0.515)	0.030(0.117)	0.225(0.881)	0.263(1.032)
		95% Cov	0.982	0.923	0.927	0.917
	LSMFM	Mean(MSE)	1.540(0.020)	0.297(0.001)	1.002(0.082)	0.987(0.102)
		SE(LCI)	0.133(0.522)	0.030(0.116)	0.273(1.070)	0.313(1.226)
		95% Cov	0.946	0.921	0.922	0.915
100	MLSM	Mean(MSE)	1.242(0.070)	0.332(0.002)	1.611(0.428)	1.977(1.035)
		SE(LCI)	0.057(0.222)	0.029(0.112)	0.228(0.894)	0.285(1.115)
		95% Cov	0.016	0.889	0.165	0.012
	LSMRM	Mean(MSE)	1.519(0.009)	0.298(0.000)	0.997(0.025)	0.993(0.035)
		SE(LCI)	0.092(0.359)	0.021(0.083)	0.159(0.623)	0.188(0.736)
		95% Cov	0.983	0.953	0.945	0.943
	LSMFM	Mean(MSE)	1.520(0.009)	0.298(0.000)	0.999(0.037)	0.995(0.049)
		SE(LCI)	0.093(0.364)	0.021(0.083)	0.192(0.754)	0.223(0.875)
		95% Cov	0.948	0.944	0.940	0.938
200	MLSM	Mean(MSE)	1.237(0.071)	0.333(0.001)	1.603(0.391)	1.966(0.974)
		SE(LCI)	0.040(0.157)	0.020(0.080)	0.160(0.629)	0.200(0.784)
		95% Cov	0.000	0.675	0.008	0.000
	LSMRM	Mean(MSE)	1.511(0.004)	0.299(0.000)	0.999(0.013)	0.994(0.018)
		SE(LCI)	0.064(0.253)	0.015(0.059)	0.113(0.441)	0.133(0.521)
		95% Cov	0.980	0.955	0.954	0.947
	LSMFM	Mean(MSE)	1.511(0.004)	0.299(0.000)	1.000(0.019)	0.995(0.025)
		SE(LCI)	0.065(0.255)	0.015(0.059)	0.136(0.533)	0.158(0.618)
		95% Cov	0.953	0.941	0.939	0.936

Presented summary statistics include the sample mean (Mean), the empirical mean squared error (MSE), the averaged standard error (SE), the averaged length of 95% confidence intervals (LCI), and estimated coverage probability for 95% confidence intervals (95% Cov)

might notice that the standard error of the estimate under the LSMRM is smaller than the ones under the LSMFM. This is expected because the LSMRM and LSMFM are mathematically equivalent when $\gamma_j = 1$ for all j , but the LSMRM has a simpler form of the likelihood function which leads to more numerically stable estimates. However, similarly to the results in the simulation section, the estimates obtained via the MLSM method suggest the monotone load-sharing rule might hold. We believe this is because the MLSM does not account for the work history.

Table 2 Simulation results for Weibull (shape = θ_1 , scale = θ_2), $\gamma_2 = 1.5$ and $\gamma_3 = 3$

n	Method	Measure	$\theta_1 = 1.5$	$\theta_2 = 0.3$	$\gamma_2 = 1.5$	$\gamma_3 = 3$
50	MLSM	Mean(MSE)	1.253(0.068)	0.331(0.002)	2.298(0.878)	5.009(5.105)
		SE(LCI)	0.081(0.318)	0.040(0.157)	0.463(1.815)	1.012(3.966)
		95% Cov	0.172	0.965	0.687	0.523
	LSMRM	Mean(MSE)	1.539(0.020)	0.297(0.001)	1.390(0.111)	2.420(0.681)
		SE(LCI)	0.133(0.522)	0.030(0.117)	0.305(1.195)	0.589(2.307)
		95% Cov	0.985	0.929	0.883	0.742
	LSMFM	Mean(MSE)	1.539(0.019)	0.297(0.001)	1.518(0.171)	3.028(0.678)
		SE(LCI)	0.133(0.522)	0.030(0.116)	0.393(1.541)	0.804(3.150)
		95% Cov	0.954	0.928	0.932	0.930
100	MLSM	Mean(MSE)	1.243(0.070)	0.332(0.002)	2.255(0.680)	4.900(4.097)
		SE(LCI)	0.057(0.223)	0.029(0.112)	0.321(1.257)	0.698(2.737)
		95% Cov	0.015	0.881	0.317	0.137
	LSMRM	Mean(MSE)	1.521(0.010)	0.298(0.000)	1.386(0.059)	2.419(0.510)
		SE(LCI)	0.093(0.364)	0.021(0.084)	0.215(0.843)	0.416(1.630)
		95% Cov	0.980	0.942	0.878	0.652
	LSMFM	Mean(MSE)	1.520(0.009)	0.299(0.000)	1.504(0.077)	3.000(0.324)
		SE(LCI)	0.093(0.364)	0.021(0.083)	0.275(1.076)	0.562(2.201)
		95% Cov	0.949	0.937	0.940	0.938
200	MLSM	Mean(MSE)	1.238(0.070)	0.333(0.001)	2.236(0.594)	4.860(3.703)
		SE(LCI)	0.040(0.157)	0.020(0.079)	0.224(0.880)	0.489(1.917)
		95% Cov	0.000	0.683	0.040	0.004
	LSMRM	Mean(MSE)	1.512(0.005)	0.299(0.000)	1.385(0.036)	2.421(0.421)
		SE(LCI)	0.065(0.256)	0.015(0.059)	0.152(0.595)	0.294(1.153)
		95% Cov	0.981	0.952	0.845	0.484
	LSMFM	Mean(MSE)	1.511(0.004)	0.299(0.000)	1.499(0.038)	2.995(0.160)
		SE(LCI)	0.065(0.255)	0.015(0.059)	0.193(0.757)	0.396(1.552)
		95% Cov	0.950	0.938	0.940	0.944

Presented summary statistics include the sample mean (Mean), the empirical mean squared error (MSE), the averaged standard error (SE), the averaged length of 95% confidence intervals (LCI), and estimated coverage probability for 95% confidence intervals (95% Cov)

To see which method performs the best in terms of modeling the reliability of the load-sharing system, we compare the prediction of the lifetime of each PDP using the obtained estimates. The lifetime of the i th PDP is S_{i3} . Using an estimate of β , we can compute an estimate of $E[S_{i3}]$, denoted by $\widehat{E}[S_{i3}]$. Then we calculated the mean prediction relative error (MRE) given by

$$\text{MRE} = \frac{1}{20} \sum_{i=1}^{20} \left| \frac{S_{i3} - \widehat{E}[S_{i3}]}{S_{i3}} \right|.$$

Table 3 Simulation results for Gamma (shape = θ_1 , rate = θ_2) and $\gamma_2 = \gamma_3 = 1$

n	Method	Measure	$\theta_1 = 2$	$\theta_2 = 10$	$\gamma_2 = 1$	$\gamma_3 = 1$
50	MLSM	Mean(MSE)	1.345(0.446)	5.729(19.44)	1.712(0.633)	1.917(0.994)
		SE(LCI)	0.121(0.474)	1.068(4.188)	0.343(1.343)	0.387(1.516)
		95% Cov	0.011	0.077	0.472	0.264
	LSMRM	Mean(MSE)	2.092(0.111)	10.790(7.10)	1.001(0.052)	0.996(0.060)
		SE(LCI)	0.304(1.193)	2.384(9.346)	0.220(0.863)	0.238(0.932)
		95% Cov	0.975	0.973	0.931	0.932
	LSMFM	Mean(MSE)	2.095(0.117)	10.796(7.45)	1.008(0.072)	1.002(0.073)
		SE(LCI)	0.310(1.217)	2.425(9.507)	0.257(1.007)	0.262(1.028)
		95% Cov	0.957	0.960	0.924	0.923
100	MLSM	Mean(MSE)	1.330(0.457)	5.577(20.09)	1.693(0.536)	1.907(0.896)
		SE(LCI)	0.084(0.330)	0.738(2.891)	0.239(0.938)	0.272(1.067)
		95% Cov	0.000	0.004	0.084	0.016
	LSMRM	Mean(MSE)	2.046(0.047)	10.373(2.81)	1.001(0.024)	1.000(0.029)
		SE(LCI)	0.209(0.821)	1.626(6.374)	0.156(0.611)	0.169(0.663)
		95% Cov	0.976	0.972	0.954	0.945
	LSMFM	Mean(MSE)	2.047(0.049)	10.375(2.90)	1.005(0.033)	1.003(0.035)
		SE(LCI)	0.214(0.837)	1.654(6.482)	0.181(0.710)	0.186(0.729)
		95% Cov	0.953	0.956	0.943	0.935
200	MLSM	Mean(MSE)	1.319(0.467)	5.496(20.53)	1.679(0.489)	1.890(0.827)
		SE(LCI)	0.059(0.231)	0.515(2.020)	0.168(0.658)	0.191(0.748)
		95% Cov	0.000	0.000	0.001	0.000
	LSMRM	Mean(MSE)	2.021(0.022)	10.178(1.38)	1.001(0.013)	0.998(0.015)
		SE(LCI)	0.146(0.572)	1.130(4.429)	0.110(0.432)	0.119(0.468)
		95% Cov	0.974	0.971	0.951	0.954
	LSMFM	Mean(MSE)	2.022(0.023)	10.180(1.43)	1.002(0.017)	0.999(0.018)
		SE(LCI)	0.149(0.583)	1.149(4.504)	0.128(0.501)	0.131(0.514)
		95% Cov	0.951	0.949	0.940	0.941

Presented summary statistics include the sample mean (Mean), the empirical mean squared error (MSE), the averaged standard error (SE), the averaged length of 95% confidence intervals (LCI), and estimated coverage probability for 95% confidence intervals (95% Cov)

The MRE results are also included in Table 5. Surprisingly, there are no significant differences among the three methods. The reason might be that each method has four parameters which give enough flexibility to capture the mean lifetime. This observation leads us to consider more informative statistics of the reliability. We proceed to consider predicting the time between two consecutive component failures; i.e., $(T_1, T_2, T_3)^T$. In real applications, with the knowledge of T_j 's, one can design a suitable maintenance procedure to keep the entire system away from completely breaking down.

Table 4 Simulation results for Gamma (shape = θ_1 , rate = θ_2), $\gamma_2 = 1.5$ and $\gamma_3 = 3$

n	Method	Measure	$\theta_1 = 2$	$\theta_2 = 10$	$\gamma_2 = 1.5$	$\gamma_3 = 3$
50	MLSM	Mean(MSE)	1.329(0.464)	5.585(20.44)	2.471(1.202)	5.324(6.572)
		SE(LCI)	0.110(0.432)	0.994(3.898)	0.499(1.956)	1.078(4.224)
		95% Cov	0.003	0.041	0.565	0.405
	LSMRM	Mean(MSE)	2.129(0.120)	10.995(7.42)	1.406(0.104)	2.532(0.548)
		SE(LCI)	0.304(1.191)	2.383(9.342)	0.303(1.186)	0.576(2.260)
		95% Cov	0.982	0.978	0.894	0.787
	LSMFM	Mean(MSE)	2.103(0.112)	10.820(6.99)	1.523(0.160)	3.015(0.613)
		SE(LCI)	0.302(1.183)	2.373(9.302)	0.384(1.504)	0.767(3.005)
		95% Cov	0.955	0.955	0.931	0.928
100	MLSM	Mean(MSE)	1.316(0.475)	5.470(20.98)	2.416(0.953)	5.241(5.532)
		SE(LCI)	0.077(0.302)	0.691(2.709)	0.344(1.350)	0.748(2.934)
		95% Cov	0.000	0.001	0.151	0.047
	LSMRM	Mean(MSE)	2.077(0.052)	10.570(3.23)	1.399(0.056)	2.543(0.377)
		SE(LCI)	0.209(0.818)	1.625(6.368)	0.213(0.835)	0.410(1.606)
		95% Cov	0.982	0.979	0.878	0.731
	LSMFM	Mean(MSE)	2.051(0.048)	10.395(2.99)	1.506(0.074)	3.013(0.298)
		SE(LCI)	0.207(0.811)	1.615(6.332)	0.268(1.049)	0.541(2.120)
		95% Cov	0.951	0.949	0.939	0.939
200	MLSM	Mean(MSE)	1.307(0.484)	5.404(21.34)	2.401(0.868)	5.183(5.013)
		SE(LCI)	0.054(0.211)	0.484(1.897)	0.242(0.948)	0.523(2.049)
		95% Cov	0.000	0.000	0.005	0.000
	LSMRM	Mean(MSE)	2.052(0.025)	10.381(1.50)	1.401(0.033)	2.540(0.294)
		SE(LCI)	0.145(0.570)	1.130(4.430)	0.151(0.591)	0.289(1.135)
		95% Cov	0.987	0.983	0.865	0.599
	LSMFM	Mean(MSE)	2.025(0.022)	10.211(1.36)	1.506(0.037)	2.995(0.147)
		SE(LCI)	0.144(0.565)	1.124(4.406)	0.189(0.740)	0.380(1.490)
		95% Cov	0.950	0.951	0.943	0.942

Presented summary statistics include the sample mean (Mean), the empirical mean squared error (MSE), the averaged standard error (SE), the averaged length of 95% confidence intervals (LCI), and estimated coverage probability for 95% confidence intervals (95% Cov)

Table 5 The plasma display device study

Method	θ_1	θ_2	γ_2	γ_3	MRE
MLSM	1.418(0.143)	10.38(1.742)	2.799(0.896)	3.420(1.083)	0.332
LSMRM	1.840(0.256)	9.189(1.213)	1.300(0.450)	1.188(0.497)	0.333
LSMFM	1.835(0.257)	9.277(1.215)	1.507(0.672)	1.229(0.680)	0.332

Presented results include the value of the MLE with an estimated standard error in the parenthesis. The last column shows the MRE results

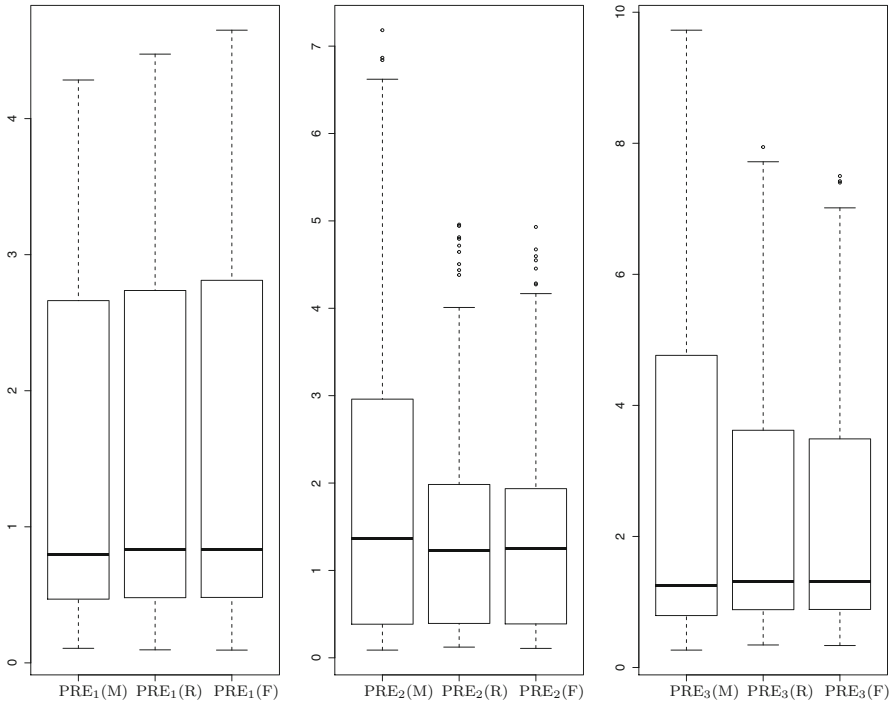


Fig. 3 The plasma display device study. Displayed figures are the boxplots of the PRE₁'s (left), PRE₂'s (middle), and PRE₃'s (right) using the MLSM, denoted by (M), the LSMRM, denoted by (R), and the LSMFM, denoted by (F)

Motivated by this, we first randomly split the data into two parts; one of size 15 as the training set and the rest 5 objects as the testing set. Using the training set, we fit the model to obtain an estimate of β . Then for each observation $(T_{i1}, T_{i2}, T_{i3})^\top$ in the testing dataset, we use the estimates to predict $E(T_{i1})$, $E(T_{i2} | T_{i1})$ and $E(T_{i3} | T_{i2}, T_{i1})$. We denote the corresponding predictions by $\hat{E}(T_{i1})$, $\hat{E}(T_{i2} | T_{i1})$ and $\hat{E}(T_{i3} | T_{i2}, T_{i1})$, respectively. The accuracy is then evaluated through the following three prediction relative errors:

$$PRE_1 = \frac{1}{5} \sum_{i=1}^5 \left| \frac{T_{i1} - \hat{E}[T_{i1}]}{T_{i1}} \right|, \quad PRE_2 = \frac{1}{5} \sum_{i=1}^5 \left| \frac{T_{i2} - \hat{E}[T_{i2} | T_{i1}]}{T_{i2}} \right|,$$

and

$$PRE_3 = \frac{1}{5} \sum_{i=1}^5 \left| \frac{T_{i3} - \hat{E}[T_{i3} | T_{i1}, T_{i2}]}{T_{i3}} \right|.$$

We performed the process of randomly splitting the data, estimating based on the training, and then predicting the testing dataset for 1000 times under all the three models.

For $j = 1, 2, 3$, denote $\text{PRE}_j(\text{M})$, $\text{PRE}_j(\text{R})$, and $\text{PRE}_j(\text{F})$ as the PRE_j obtained using the MLSM, LSMRM, and LSMFM, respectively. In Fig. 3, we present the boxplot of the 1000 values of $\text{PRE}_j(\text{M})$, $\text{PRE}_j(\text{R})$, and $\text{PRE}_j(\text{F})$, for $j = 1, 2, 3$. One can see that in terms of predicting T_{i1} , three methods basically performed the same. The difference between the LSMRM and LSMFM is minimum. The result is reasonable since our point estimates of $\boldsymbol{\gamma}$ indicate $\gamma_2 = \gamma_3 = 1$, in which case, the models LSMRM and LSMFM become the same. In terms of predicting the second component failure given the first failure time; i.e., $E(T_{i2} | T_{i1})$, both the LSMRM and LSMFM perform better than the MLSM. For $E(T_{i3} | T_{i2}, T_{i1})$, both the LSMRM and LSMFM produce more robust prediction. These results indicate that, with the consideration of previous working time, both LSMRM and LSMFM are able to produce more informative prediction than the traditional memoryless models.

7 Discussion

In this article, we believe that after each component failure, the changes in the hazard rate of functioning components come from the redistribution of the total load and also the work history. The fact that traditional load-sharing models do not take account of the work history motivated us to consider a general framework of load-sharing models with memory. We have discussed potential researches within this general framework by using the “self-exciting” idea of Hawkes processes and the Cox proportional hazard models in Sect. 2. Then we proposed two classes of load-sharing models with memory: the LSMRM and the LSMFM. The maximum likelihood estimator is developed. We carried out extensive Monte Carlo simulations and analyzed a real data example to illustrate the new methods. We would like to point out that, instead of using the Hessian matrix, one could also study the generalized pivotal quantity (Weerahandi 1993) to improve the accuracy of confidence interval estimation. This could be an interesting future topic. Moreover, we did not consider the model selection between the two models with memory or any kind of goodness-of-fit testing, all of which could be interesting topics along with this research avenue. Our mainly study herein is to compare the proposed models with the traditional memoryless models. One important message from our study is that, if one applied an memoryless model and the resulting estimates implied a monotone load-sharing rule, it might be due to the neglect of the work history.

Throughout the article, we assume that the load is equally distributed to functioning components and the entire system works till the last component fails. For future investigations, the load-sharing models with memory can also be studied under a local load-sharing rule; i.e., components closer to the failed one undertake more load, or when the system fails if k out of J components failed. Furthermore, one could also consider that the load-sharing system keeps expanding along with the time; for example, more generators are added in a power plant or more computers are connected in a computing system. In these applications, the number of components actually increases with time. Finally, our real data analysis reveals an interesting result; i.e., when the system is not memoryless, the memory could help build informative prediction for all the failure moments. Motivated by these observations, an attractive future topic could be

to build up a cost-effective maintenance plan for large complex load-sharing systems by considering work history.

Acknowledgements This work was partially supported by the National Research Foundation of Korea (NRF) grant funded by the Korea government (No. NRF-2017R1A2B4004169). We would like to thank an Associate Editor and two anonymous referees for their constructive suggestions that have greatly improved the presentation of this article.

Appendix

We present the regularity conditions for the asymptotic properties of $\widehat{\beta}_n$ in Theorem 1.

(A1) The model $f(T_1, \dots, T_J \mid \beta)$ has a common support and is identifiable; i.e., $f(T_1, \dots, T_J \mid \beta_1) = f(T_1, \dots, T_J \mid \beta_2)$ if and only if $\beta_1 = \beta_2$. Furthermore, the first and second derivatives of $\log f$ satisfy the equations

$$E_{\beta} \left[\frac{\partial \log f(T_1, \dots, T_J \mid \beta)}{\partial \beta} \right] = \mathbf{0}$$

and

$$\begin{aligned} & E_{\beta} \left[-\frac{\partial^2 \log f(T_1, \dots, T_J \mid \beta)}{\partial \beta \partial \beta^{\top}} \right] \\ &= E_{\beta} \left[\frac{\partial \log f(T_1, \dots, T_J \mid \beta)}{\partial \beta} \frac{\partial \log f(T_1, \dots, T_J \mid \beta)}{\partial \beta^{\top}} \right]. \end{aligned}$$

(A2) The Fisher information matrix

$$\mathcal{I}(\beta) = E_{\beta} \left[\frac{\partial \log f(T_1, \dots, T_J \mid \beta)}{\partial \beta} \frac{\partial \log f(T_1, \dots, T_J \mid \beta)}{\partial \beta^{\top}} \right]$$

is finite and positive definite at β_0 .

(A3) Denote the parameter space for β by Ω . There exists an open subset $\omega \subset \Omega$ such that $\beta_0 \in \omega$ and $\partial^3 f(T_1, \dots, T_J \mid \beta) / (\partial \beta_{l_1} \partial \beta_{l_2} \partial \beta_{l_3})$ exists for $\beta \in \omega$ and almost all (T_1, \dots, T_J) . In addition, there exist functions M_{l_1, l_2, l_3} such that

$$\left| \frac{\partial^3 f(T_1, \dots, T_J \mid \beta)}{\partial \beta_{l_1} \partial \beta_{l_2} \partial \beta_{l_3}} \right| \leq M_{l_1, l_2, l_3}(T_1, \dots, T_J)$$

where $E_{\beta_0}[M_{l_1, l_2, l_3}(T_1, \dots, T_J)] < \infty$ for all l_1, l_2, l_3 .

These regularity conditions guarantee the asymptotic normality of the maximum likelihood estimator (Lehmann 1983). The proof of Theorem 1 is standard and hence omitted.

References

- Aït-Sahalia Y, Cacho-Diaz J, Laeven R (2015) Modeling financial contagion using mutually exciting jump processes. *J Financ Econ* 117:585–606
- Birnbaum Z, Saunders S (1958) A statistical model for life length of material. *J Am Stat Assoc* 53:151–160
- Coleman B (1957a) Time dependence of mechanical breakdown in bundles of fibers I. Constant total load. *J Appl Phys* 28:1058–1064
- Coleman B (1957b) Time dependence of mechanical breakdown in bundles of fibers II. The infinite ideal bundle under linearly increasing loads. *J Appl Phys* 28:1065–1067
- Cox D (1972) Regress models and life-tables. *J R Stat Soc Ser B* 34:187–220
- Daniels H (1945) The statistical theory of the strength of bundles of threads I. *Proc R Soc A* 83:405–435
- Durham S, Lynch J, Padgett W, Horan T, Owen W, Surles H (1997) Localized load-sharing rules and Markov–Weibull fibers: a comparison of microcomposite failure data with Monte Carlo simulations. *J Compos Mater* 31:1856–1882
- Fonseca J, Zaatour R (2014) Hawkes process: fast calibration, application to trade clustering, and diffusive limit. *J Futures Mark* 34:548–579
- Harlow D (1997) Statistical properties of hybrid composites: asymptotic distributions for strain. *Reliab Eng Syst Saf* 56:197–208
- Harlow D, Phoenix S (1978) The chain-of-bundles probability model for the strength of fibrous materials I. Analysis and conjectures. *J Compos Mater* 12:195–214
- Hawkes A (1971) Spectra of some self-exciting and mutually exciting point processes. *Biometrika* 58:83–90
- Hawkes A, Adamopoulos L (1973) Cluster models for earthquakes-regional comparisons. *Bull Int Stat Inst* 45:454–461
- Kim H, Kvam P (2004) Reliability estimation based on system data with an unknown load share rule. *Lifetime Data Anal* 10:83–94
- Kvam P, Peña E (2005) Estimating load-sharing properties in a dynamic reliability system. *J Am Stat Assoc* 100:262–272
- Lee S, Durham S, Lynch J (1995) On the calculation of the reliability of general load sharing system. *J Appl Probab* 32:777–792
- Lehmann E (1983) *Theory of point estimation*. Wadsworth and Brooks/Cole, Pacific Grove
- Mohler G, Short M, Brantingham P, Schoenberg F, Tita G (2011) Self-exciting point process modeling of crime. *J Am Stat Assoc* 106:100–108
- Nelson W (1980) Accelerated life testing - step-stress models and data analyses. *IEEE Trans Reliab* 29:103–108
- Ogata Y (1998) Space-time point-process models for earthquake occurrences. *Ann Inst Stat Math* 50:379–402
- Park C (2010) Parameter estimation for the reliability of load-sharing systems. *IIE Trans* 42:753–765
- Park C (2013) Parameter estimation from load-sharing system data using the expectation-maximization algorithm. *IIE Trans* 45:147–163
- Phoenix S (1978) The asymptotic time to failure of a mechanical system of parallel members. *SIAM J Appl Math* 34:227–246
- Phoenix S, Tierney L (1983) A statistical model for the time dependent failure of unidirectional composite material under local elastic load-sharing among fibers. *Eng Fract Mech* 18:193–215
- Rosen B (1964) Tensile failure of fibrous composites. *AIAA J* 2:1985–1991
- Singh B, Sharma K, Kumar A (2008) A classical and Bayesian estimation of a k-components load-sharing parallel system. *Comput Stat Data Anal* 52:5175–5185
- Weerahandi S (1993) Generalized confidence intervals. *J Am Stat Assoc* 88:809–905
- Zhao W, Elsayed E (2005) A general accelerated lifemodel for step-stress testing. *IEE Trans* 37:1059–1069